Acid-Catalyzed Chitin Liquefaction in Ethylene Glycol

Yann Pierson,[†,‡] Xi Chen,[†] Felix D. Bobbink,[†,‡] Jiaguang Zhang,[†] and Ning Yan*,[†]

[†]Department of Chemical and Biomolecular Engineering, National University of Singapore, 4 Engineering Drive 4, 117585 Singapore
[‡]Institut des Sciences et Ingénierie Chimiques, Ecole Polytechnique Fédérale de Lausanne (EPFL), 1015 Lausanne, Switzerland

Ⓢ Supporting Information

ABSTRACT: This paper describes chitin liquefaction in ethylene glycol (EG) under the catalysis of sulfuric acid for the first time. Up to 75% of chitin was liquefied at 165 °C within 90 min by using 8 wt % of acid (refer to the mass of EG). The major products (30% yield) were identified to be hydroxyethyl-2-amino-2-deoxyhexopyranoside (HADP) and hydroxyethyl-2-acetamido-2-deoxyhexopyranoside (HAADP) by GC-MS and confirmed by NMR. Kinetic studies were conducted based on which a plausible mechanism for product formation was proposed. HADP was dominant during the reaction, whereas HAADP formed fast at an initial stage and then most of it was hydrolyzed to HADP. Unreacted chitin residues with different reaction times were characterized by Fourier transform infrared spectroscopy (FTIR), X-ray powder diffraction (XRD), and solid state NMR. The FTIR results showed that negligible deacetylation reaction occurred, supporting the assumption that HADP was produced from the hydrolysis of HAADP rather than directly from chitin polymer chains. The XRD analysis revealed the gradual decrease in crystallinity with the increase in reaction time, indicating the damage of the crystalline domain by the liquefaction process. The simple, cheap, and efficient liquefaction of chitin opens up a new route to produce chemicals and materials from waste in the fishing industry.

KEYWORDS: Chitin, Liquefaction, N-containing chemical, Polyol, Biomass
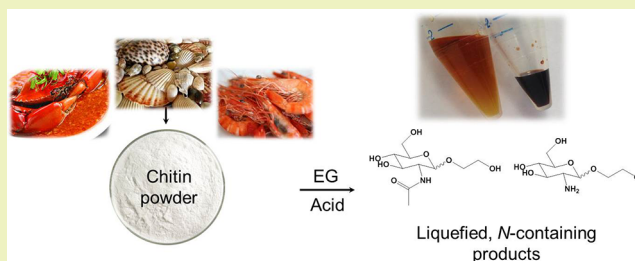
■ INTRODUCTION

In a time marked by slow but continued fossil fuel depletion, as well as the rise of ecological consciousness, biomass utilization[1,2] draws remarkable research interests. Biomass represents an alternative sustainable resource for the manufacture of biofuels and value-added chemicals.[3−6] Lignocellulosic materials, comprising cellulose,[7−12] hemicellulose,[13] and lignin[14−17] components, attracted the most scientific attention in the past decades. Among the various transformation strategies for lignocellulosic biomass, liquefaction process[18,19] is a simple and effective method to convert solid biomass into liquid polyols or aromatics that can be directly used to produce value-added polymers.[20−24] The liquefaction process is usually conducted under atmospheric pressure at elevated temperatures by using polyhydric alcohols as the solvent and acids as the catalyst.[25,26] Under the catalysis of acids, the polymer chain is solvolyzed and depolymerized by the solvent molecules. Liquefaction of cellulose,[27] lignin,[28,29] and even wood[30] has already been reported using polyethylene glycol (PEG),[31] EG,[32] or glycol[33] as the solvent.[34] For acid-catalyzed liquefaction, the temperature used is usually between 150 and 170 °C with liquefaction efficiency from 60% to 100% for various lignocellulosic biomass substrates. Sulfuric acid is the most commonly used acid catalyst. It is reported that cellulose liquefaction in EG at 150 °C catalyzed by sulfuric acid afforded mainly EG-glucosides and its decomposed compound 2-hydroxyethyl levulinate as the product. A proposed mechanism suggested that EG-glucosides were formed initially through solvolytic reactions, after which decomposition reaction occurred to form the major product levulinate esters.[27]

So far, the liquefaction process is largely limited to land-based lignocellulosic materials,[35,36] whereas the expansion for processing a wider range of biomass is desirable and beneficial. Chitin, which is the world's second most abundant biomass close to cellulose,[37] holds a great but underestimated potential for biochemical and biomaterial production.[38] Chitin is a major component of the exoskeletons of insects and crustaceans consisting of N-acetyl-D-glucosamine (NAG) monosaccharide produced mainly from shellfish wastes in the fishing industry (Figure 1). Their current application remains limited, such as wound healing enhancer,[39] enzyme immobilization,[40] drug release control,[41] industrial pollutants treatment,[42] and formation of films.[43] The conventional transformation strategies of chitin include chemical modification,[44] pyrolysis,[45] and hydrolysis.[46−48] Due to the 7 wt % biologically fixed nitrogen, chitin offers an overlooked but significant potential for sustainable production of nitrogen-containing (N-containing) chemicals or materials. The structure of chitin (Figure 1) is very similar to cellulose with the only difference on the C2 position (acetyl amide side chain instead of hydroxyl group). Previously,
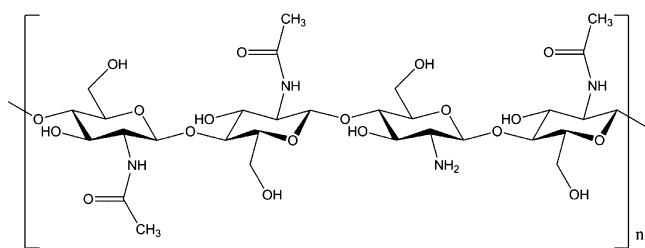
Figure 1. Chemical structure of chitin polymer.

cellulose was liquefied to produce polyols and further transformed into polyurethanes foams (PUFs)[49] and other materials.[50,51] It is not unreasonable then to speculate that the liquefaction process established for cellulose is applicable to chitin utilization, through which chitin can be transformed into small molecules with both hydroxyl and amine/amide groups. These intermediate compounds can be processed into PUFs and even polyamides. We envisage that the establishment of chitin liquefaction will contribute to the current scheme of NAG/chitin utilization,[52−56] providing a bridge to transform wastes into valuable chemicals/materials.

In this paper, the liquefaction of chitin was conducted by using EG as the solvent and various acids as the catalyst. Up to 75% of chitin was successfully converted into liquid products at 165 °C after 90 min in the presence of sulfuric acid. Product identification showed that the major products are HADP and HAADP with a total yield of about 30%. Kinetic studies and NMR analysis of the liquefied products have been conducted. Moreover, recovered chitin solid after the reaction has been characterized to probe structural changes during reaction. Finally, a plausible liquefaction mechanism of chitin is proposed based on kinetic studies and previous reports on cellulose liquefaction.

■ EXPERIMENTAL SECTION

Materials. Chitin (white powder) was purchased from Wako Pure Chemical Industries. Hexamethyldisilazane (HMDS), trifluoreacetic

acid, pyridine, N-acetyl-D-glucosamine (NAG, 99%), and D-glucosamine hydrochloride (Glu, >99%) were obtained from Sigma-Aldrich. Ethylene glycol (EG, >99%) and phosphoric acid (85%) were purchased from VWR Singapore company. Sulfuric acid (96.9%) was purchased from J. T. Baker. Hydrochloric acid (37%) and acetic acid (99%) were obtained from Merck. These chemicals and all solvents used in this study were of reagent grade and were used as received.

Characterization. XRD was performed on a Bruker D8 advanced diffractometer with Cu Kα radiation at 40 kV. The XRD instrument was calibrated by using standard reference material (SRM). The equation for the crystalline index (CI) calculation is shown below.[57]

$$\mathrm{CI}\ (\%) = \left[\frac{I_{110} - I_{am}}{I_{110}} \right] \times 100$$

where I_{110} is the maximum intensity of the diffraction for the (110) plane at approximately $2\theta = 19.2°$, and I_{am} is the intensity of the amorphous diffraction at approximately $2\theta = 12.7°$.

FTIR was conducted on a Bio-Rad FTS-3500 ARX instrument. The DA was calculated using FTIR spectra.[58] Specifically, the DA is proportional to the ratio of A_{1660}/A_{3450}, where A_i is the area of the peak at wavenumber i. In order to prevent the error from drawing the baselines, original chitin was used as a reference, which has 99% DA as demonstrated previously.[55] 1D and 2D NMR analysis was performed on a Bruker ultrashield 400 plus spectrometer. The samples were prepared using D_2O as the solvent. The calibration of the NMR signal was conducted by using tetramethylsilane (TMS) as a standard. Solid-state NMR was conducted on a Bruker Avance 400 (DRX400) with CP/MAS.

HPLC separation was achieved by using an Agilent 1200 series (Agilent Technologies, Germany) LC system by using an Agilent Hi-Plex Ca sugar column. The mobile phase was 100% water. The flow rate was kept at 0.6 mL/min with a run time of 20 min at 80 °C. An UV−vis detector setting at 210 nm was used to analyze the product. To isolate the major products, 20 injections (each time 20 μL) were performed, and each fraction was accumulatively collected.

NAG Reaction Procedure. In a Schlenk tube equipped with a cooling device and a stirrer, chemicals were added in the order of EG (1 g), sulfuric acid (0.08 g, 8% w/w EG), and NAG (0.15 g, 15% w/w EG). The reaction mixture was heated to 120 °C and allowed to react for a desired period of time. After the reaction, it was cooled to 0 °C and neutralized with aqueous NaOH (10 wt %). The water in the
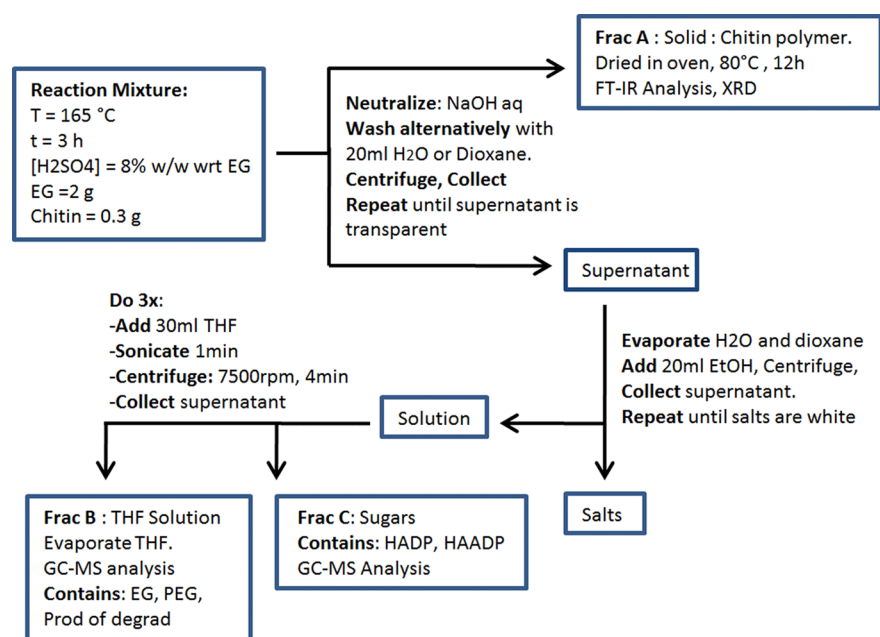

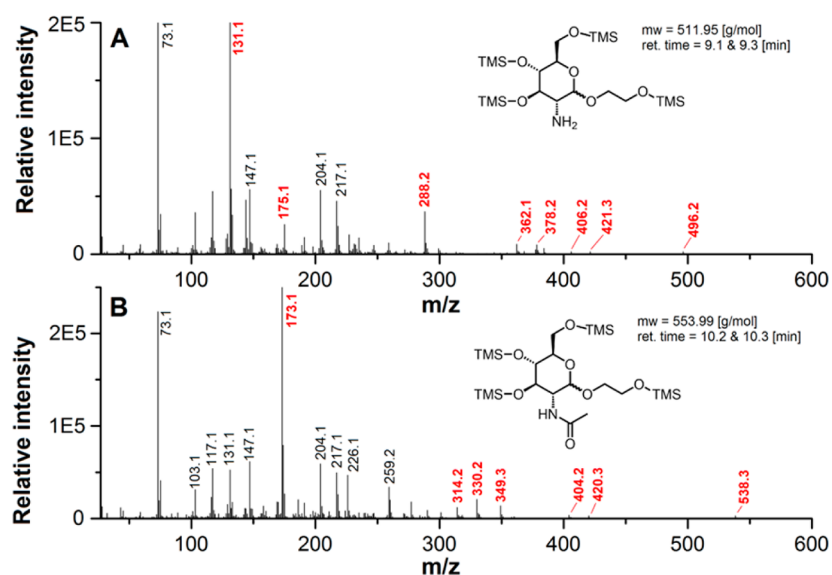**Figure 2.** Flow diagram of product separation in chitin liquefaction.

Figure 3. MS spectra of HADP (A) and HAADP (B). Reaction conditions: 1g of EG, 0.08 g of sulfuric acid (8% w/w EG), and 0.15 g of NAG (15% w/w EG) at 120 °C.

solution was removed by freeze-drying. Next, EtOH (15 mL) was added to the remaining solid. The salt was removed as an insoluble precipitate by centrifugation. Finally, the EtOH solvent was removed over a rotary evaporator to obtain the products.

Chitin Liquefaction Procedure. The chitin liquefaction process is summarized graphically in Figure 2 and is executed as follows. In a Schlenk tube equipped with a cooling device and a stirrer, chemicals were added in the order of EG (2 g), sulfuric acid (0.16 g, 8% w/w EG), and chitin (0.3 g, 15% w/w EG). The reaction mixture was heated to 165 °C and allowed to react for a desired period of time. Chitin is more difficult to convert than NAG, and a higher reaction temperature was employed. After the reaction, the tube was cooled to 0 °C and neutralized with aqueous NaOH (10 wt %). For product identification, fractionation procedures were taken. To obtain unreacted chitin, the solution was centrifuged at 7500 rpm for 4 min. The residual solid (Fraction A) was sequentially washed and centrifuged with a water (dioxane is also effective) solution (20 mL) and dried in an oven at 80 °C for 12 h. Meanwhile, the supernatant was evaporated, and EtOH (20 mL) was added. The salts from neutralization were removed by centrifugation. Next, the EtOH solution was removed over a rotary evaporator, and THF was added to purposely remove the large amount of EG solvent. Upon the addition of THF, two layers formed with THF as the upper layer and a brown oil as the lower layer. The upper THF layer was evaporated to obtain a yellow solution denoted as Fraction B. The brown oil was collected and denoted as Fraction C. In further analysis, it was proven that the solvent has been largely concentrated in Fraction B. For the calculation of chitin conversion, the following equation was used.

$$\text{Conversion} = \frac{\text{Starting chitin (mg)} - \text{Residual solid (mg)}}{\text{Starting chitin (mg)}} \times 100$$

Silylation Procedure for GC-MS Analysis. Products from chitin liquefaction and NAG reaction were identified with gas chromatography–mass spectrometry (GC-MS). GC-MS was performed on an Agilent 7890A GC system with a 7693 Autosampler, 5975C inert MSD with triple-axis detector, and an Agilent HP-5 column. To identify polyols on GC-MS, silylation was used to derivatize the hydroxyl groups of the products to trimethylsilyl groups to make them thermally stable.[59] A general procedure was as follows. In an analytical vial (1 mL), the product mixture to be analyzed (40 mg), pyridine (700 μL), hexamethyldisililazane (700 μL), trifluoreacetic acid (TFA, 60 μL), and a small stirring bar were added. The closed vial was put in a water bath at 60 °C for 1 h. After silylation, a portion of the reaction mixture (250 μL) and diethyl ether (750 μL) were mixed together and

analyzed by GC-MS. The GC program is as follows. The initial temperature was set to 100 °C, with an increase of 20 °C/min to 280 °C with a final hold of 3 min.

Quantification of Major Products. Because the major products HADP and HAADP were not commercially available, the quantification was conducted on an Agilent 7890A GC with a flame ionization detector (FID) and Agilent HP-5 column by employing *n*-dodecane as the internal standard. The yield was calculated by using the effective carbon numbers.[60]

■ RESULTS AND DISCUSSION

Preliminary Work on NAG Model Compound. NAG is the monosaccharide of chitin polymer; an initial attempt by using NAG as the starting material simplifies the identification of products and the establishment of reaction protocols. The liquefaction of NAG was conducted at 120 °C. As the products are mainly at high boiling point thermally unstable polyols, direct analysis by GC-MS is not possible. Prior to analysis, the silylation method was employed to transform these polyols to stable silylated chemicals that could be analyzed on GC-MS.

On the GC-MS spectra, several solvent peaks were identified as EG, EG dimer, trimer, and tetramer and were further confirmed by a blank experiment (Figure S1, Supporting Information). The side products were formed by the intermolecular condensation of EG in the presence of acid. There are several major peaks arising in the middle range (7–10.5 min) of the GC spectrum (Figure 7), which could not be recognized by the MS database. Nevertheless, their MS spectra (Figure 3) were carefully examined, and two compounds, EG-derived NAG (HAADP) and glucosamine (HADP), can be assigned satisfactorily. In the MS spectra, the peaks labeled in red indicate the fragments bearing silica, whereas the peaks labeled in black represent fragments without silica. The formation pathways of these peaks are shown in Figures 4 and 5, which are in agreement with those of the silylated carbohydrates reported previously.[61] For HAADP, the peak at *m/z* 553.3 is the molecular peak. By losing one of the methyl groups, the M-15 peak appeared at *m/z* 538.3 (Figure 4A). The peaks at *m/z* 420.2 and 404.2 resulted from the loss of silylated EG moiety. By further losing the trimethylsilanol group, the peaks at *m/z* 330.2 and 314.1 were generated (Figure 4A,B). A
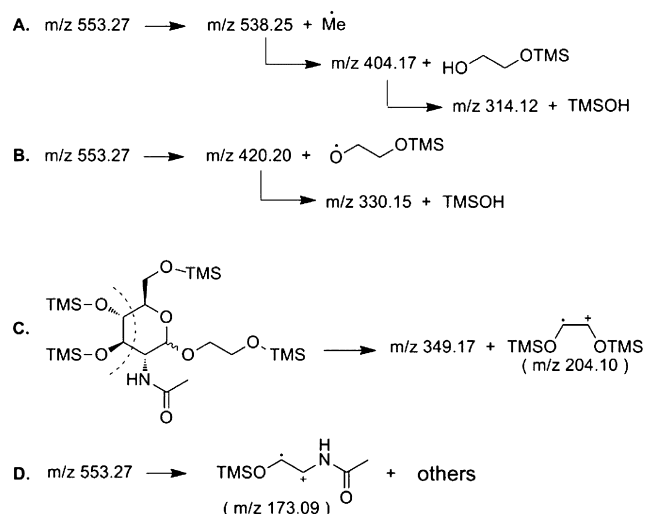
Figure 4. Proposed fragmentation pathways for product HAADP.

Figure 6. ^{13}C NMR spectrum of HAADP (α-anomer) after HPLC purification of the raw product. Reaction conditions: 1g of EG, 0.08 g of sulfuric acid (8% w/w EG), and 0.15 g of NAG (15% w/w EG) at 120 °C for 5 min. Chemical shift from left to right: δ 174.5, 97.2, 71.9, 71.2, 70.0, 68.9, 60.7, 60.6, 53.6, 21.9. The inserted magnified figure shows two adjacent peaks around 60 ppm.

third fragmentation pathway (Figure 4C) lead to m/z peaks at 349.2 and 204.1. A strong peak at m/z 173.1 may be ascribed to the silylated acetamido moiety, despite that the fragmentation pathway is not clear (Figure 4D). In a similar way (Figure 5), all major peaks in Figure 3B can be rationalized as fragments from HADP. As a result, the compounds at 8.4, 9.1, and 9.3 min were assigned to HADP, and compounds at 10.2 and 10.3 min were assigned to HAADP. The multi-peaks are caused by the formation of isomers during silylation, which is not uncommon in the silylation of sugars.[62]

To further substantiate the structure of the products, especially the position of the EG group, preparative HPLC was used to purify the product (NAG as starting material, 5 min reaction time), followed by NMR analysis. Two major fractions (1 and 2) were collected. The ^{13}C NMR spectrum of Fraction 1 is shown in Figure 6, which unambiguously confirmed the structure to be HAADP (α-anomer). Compared with the NAG standard sample (α-anomer, Figure S2, Supporting Information), two new peaks arise at 60.66 and 60.61 ppm, which indicated the formation of an EG-derived compound. The C1
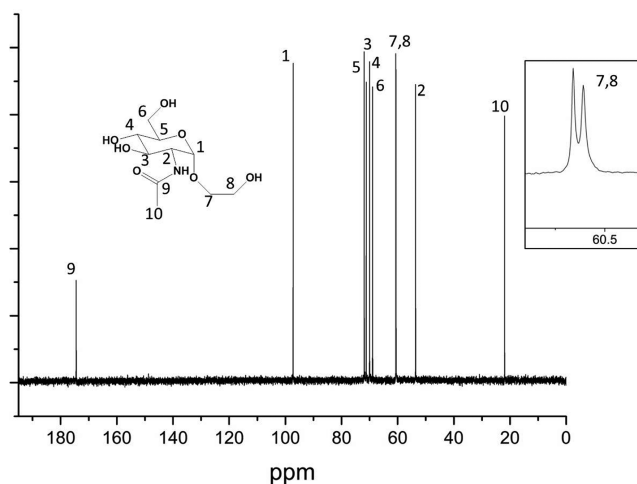
signal exhibited a downfield shift from 91.0 ppm in NAG (α-anomer) to 97.2 ppm in the product, suggesting the EG moiety is connected with C1. Fraction 2 contains a mixture of α-anomer and β-anomer from ^{13}C NMR spectrum analysis (Figure S4, Supporting Information). As such, the NMR study is in fully agreement with GC-MS identification. ^{13}C NMR analysis of the NAG standard and Fraction 2, as well as ^1H NMR spectra of both Fraction 1 and 2, are provided in Figures S2−S4 of the Supporting Information.

After successful identification of the liquefied products, reactions with durations from 5 to 100 min were carried out by using NAG as the substrate at 120 °C. The results (Figure 7) show that HAADP was formed very quickly within 5 min. At 10 min, the peaks of HAADP were significantly reduced, and the peaks of HADP increased. With a further increase in time, the signals of HADP keep climbing gradually. This observation suggested that HAADP was produced initially by solvolysis, and
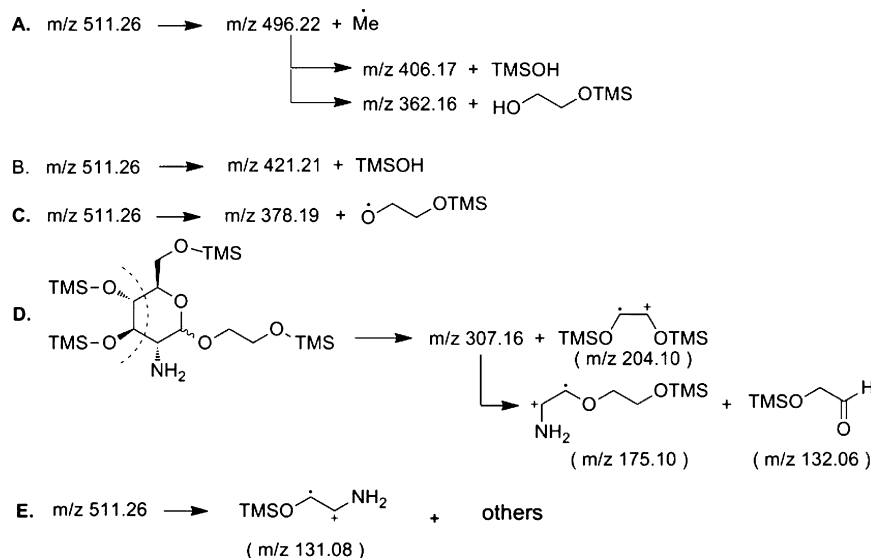

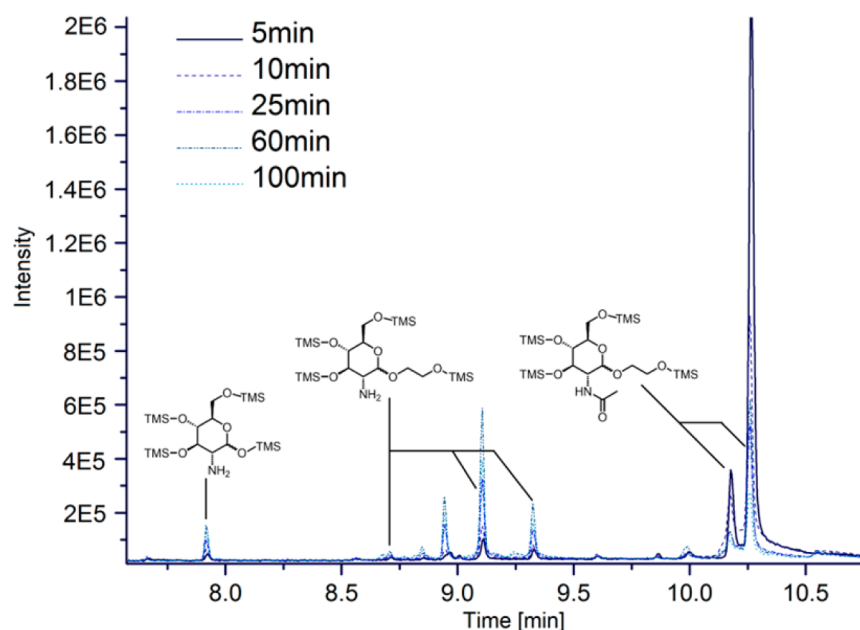**Figure 5.** Proposed fragmentation pathways for product HADP.

Figure 7. GC-MS spectra of NAG reaction with different reaction times. Peaks are labeled and assigned to HAADP and HADP accordingly. Reaction conditions: 1 g of EG, 0.08 g of sulfuric acid (8% w/w EG), and 0.15 g of NAG (15% w/w EG) at 120 °C.

then the acetyl amide side chain hydrolyzed to form HADP. These preliminary tests using NAG provide valuable information on product identification and the reaction pathway for chitin liquefaction.

Chitin Liquefaction. Chitin liquefaction was conducted in the next step. Different acid catalysts were evaluated, including sulfuric acid, hydrochloric acid, phosphoric acid, and acetic acid at 165 °C. The reaction temperature is higher than NAG conversion because chitin is more complex and inert. Table S1 of the Supporting Information shows the chitin conversion into liquefied products with different acids. Sulfuric acid was most effective—enabling a chitin conversion of 63.5%—whereas all other acids resulted in 10−30% conversion. This observation is consistent with previous reports[63] that concentrated sulfuric acid exhibits the highest catalytic ability in lignocellulosic biomass liquefaction. It is expected that sulfuric and hydrochloric acids are more effective than phosphoric and acetic acids because of their stronger acidity. The relatively lower efficiency of hydrochloric acid is ascribed to the high water content, which may have a negative effect on chitin swelling and liquefaction. The optimal acid loading is 8 wt %, which maintains satisfactory liquefaction efficiency and avoids detrimental side reactions due to high loading of acid.

Due to the complexity of chitin liquefaction products, fractionation procedures were employed for post-treatment. Centrifugation was the first step to use, through which unreacted chitin material can be recovered as a solid, denoted as Fraction A. After neutralization of the solution and removing the salt, the products are further fractionated into two portions by THF, i.e., a light yellow liquid fraction that is THF soluble, denoted as Fraction B, and a brown viscous liquid fraction that is THF insoluble, denoted as Fraction C. Under standard conditions (8 wt % sulfuric acid, 165 °C, 1 h), the weight ratio among Fractions A, B, and C, roughly, is 1:13:2.5. The total mass of the three fractions is much larger than the feeding chitin due to the facts that (1) Fraction B mostly comprises EG and EG oligomers and (2) EG is chemically bonded to fragments from chitin (vide infra).

Fraction A. Recovered solid (Fraction A) was characterized by XRD, FTIR, and solid state NMR analysis, and it was identified as unreacted chitin. Figure 8 shows the XRD pattern
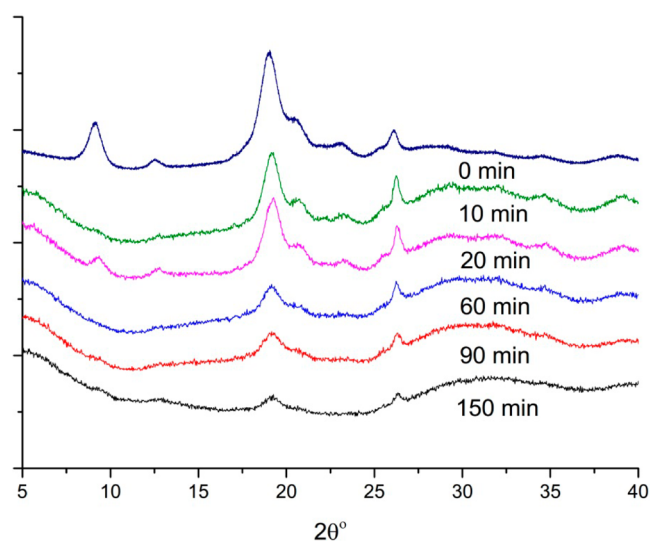

Figure 8. XRD spectra of chitin residues with different liquefaction time. Reaction conditions: 2 g of EG, 0.16 g of sulfuric acid (8% w/w EG), and 0.3 g of chitin (15% w/w EG) at 165 °C.

of residual chitin with different reaction times, which clearly demonstrates the evolution of the chitin crystal structure. With an increase in reaction time, the major peak at $2\theta = 19°$, which represents the (110) plane of crystalline chitin, decreased dramatically. Table 1 shows the calculated CI values of recovered solids. Pure chitin has a CI value of 90.3%. After 10 min of reaction, the CI value of chitin was 92.4%, essentially the same as the starting material, indicating that the crystallinity of chitin did not decrease within such a short period of time. As the reaction proceeded, an obvious decrease in the CI values was observed. Apparently, the crystallinity of chitin dropped

Table 1. Calculated CI Values of Chitin Residues with Different Liquefaction Times[a]

time (min)	0	10	20	60	90	150
CI (%)	90.3	92.4	83.5	85.0	79.0	65.5

[a]Reaction conditions: 2 g of EG, 0.16 g of sulfuric acid (8% w/w EG), and 0.3 g of chitin (15% w/w EG) at 165 °C.

significantly after long-time reactions. The chitin crystalline domain is very difficult to access due to the strong hydrogen bond network. The XRD analysis suggested that our liquefaction process is highly effective in breaking down the crystalline region in chitin.

FTIR analysis (Figure S5, Supporting Information) was used to characterize the residual solids collected after different reaction times. The bands at about 3492 and 3262 cm^{-1} represent OH and NH stretching, and the bands at about 2890 to 2965 cm^{-1} are assigned to CH, CH$_3$ symmetric stretching, and CH$_2$ asymmetric stretching, respectively. The peaks at 1629 and 1661 cm^{-1} are assigned to Amide I band, while Amide II and III bands appear at 1558 and 1312 cm^{-1}, respectively. Besides, the asymmetric bridge oxygen and C−O stretching bands show up from 1024 to 1163 cm^{-1}.[64,65] On the basis of the analysis, the recovered chitin maintained the chemical backbone of chitin. The calculated DA values for recovered solids with different reaction times are shown in Table S2 of the Supporting Information. Note that some of the results are higher than 100%, which is also observed in the literature.[58] However, the errors were all within 5%, and it is not unreasonable to conclude that negligible deacetylation occurred during the liquefaction. This indicates that the hydrolysis of the acetyl amide group happened after depolymerization. Possibly, the liquefaction happened from chitin depolymerization and released EG-derived NAG monomer or oligomers. Afterward, the side chain hydrolyzed to form EG-derived glucosamine.

^{13}C Solid-state NMR measurements on fresh chitin and the recovered solid sample were conducted to corroborate FTIR and XRD analysis (Figure S6, Supporting Information). The position and relative intensity of the peaks are identical between the two samples, indicating no appreciable change in the chemical structure in the remaining chitin. On the other hand, the peaks become shaper and more intensified in the recovered chitin after reaction, which indirectly reflects that the degree of polymerization has decreased after the liquefaction.

Fraction B and C. Fraction B and C were analyzed by GC-MS, and the major products were identified in a similar way as described in the NAG reaction. As shown in the GC-MS spectra (Figure S7, Supporting Information), Fraction B contains mainly the solvent EG, EG oligomers, and 2-hydroxyethyl acetate, which resulted from the hydrolysis and liquefaction of the acetyl amide group and also a minor amount of HADP and HAADP. Fraction C contains mainly HADP and HAADP products. Both HADP and HAADP exhibited a few peaks in the spectra, which are due to the formation of different isomers after silylation as mentioned above.

In order to obtain the kinetic profile, both samples of Fractions B and C with different reaction times were analyzed by GC-FID. Figure 9 shows the chitin conversion, yields of HADP and HAADP with different reaction times. An amount of 25% of chitin was liquefied within the first 10 min (Figure 9). Afterward, the rate became slower, and the conversion reached a maximum of 75% within 90 min. Further prolonging the
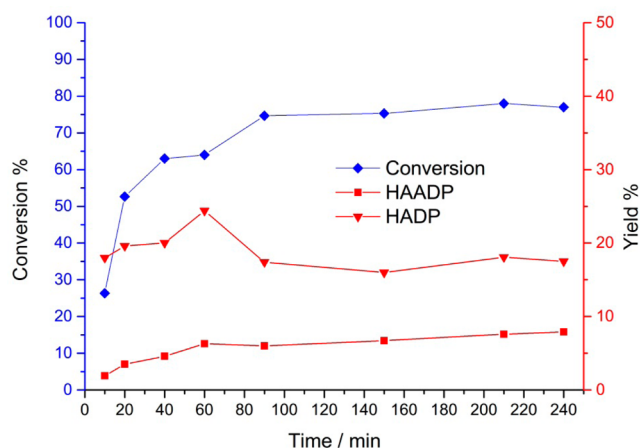

Figure 9. Chitin conversion and HADP and HAADP yields with different reaction times. Reaction conditions: 2 g of EG, 0.16 g of sulfuric acid (8% w/w EG), and 0.3 g of chitin (15% w/w EG) at 165 °C.

reaction time beyond 90 min did not result in any improvement of conversion, despite the fact that the chitin crystallinity kept decreasing. In the literature, liquefaction of woody biomass is often featured by a rapid rate within the first 30 min and then a much slower rate[66,67] because an amorphous region of biomass converts much faster, which leads to a high initial liquefaction rate. In chitin liquefaction, the situation is more complicated. The kinetics show that HADP was the major product with a maximum yield of 23.8% after 60 min. Note HADP contains one amine group that readily reacts with sulfuric acid. As such, the catalytic system deactivates as HADP accumulates with time.

1D and 2D NMR analyses were conducted on Fraction C by using samples after 60 and 90 min reactions. ^{1}H and ^{13}C NMR spectra are shown in Figure S8 of the Supporting Information. The most prominent peaks in the ^{1}H and ^{13}C NMR spectra were assigned to EG, the solvent of liquefaction, which was not completely removed in the fractionation procedure. EtOH and THF peaks were also observed. In addition to these, a number of peaks appeared between 50 and 80 ppm in the ^{13}C NMR spectra. Correspondingly, a series of peaks between 3 and 4.2 ppm in ^{1}H NMR spectrum were observed. These peaks were ascribed to the liquefied products HADP and HAADP. The CH−OH groups from the pyranose structure usually showed similar signals in this range.[27,55] 2D Heteronuclear multiple-quantum correlation spectroscopy (HMQC) NMR was conducted in an attempt to obtain more information, but the peaks from EG and its oligomers complicate the assignment (Figure S9, Supporting Information).

Proposed Mechanism for Chitin Liquefaction. The mechanism of cellulose liquefaction has been proposed previously.[9,12,15,36] It was assumed that EG-derived glucose units were formed initially, and then decomposition happened, affording levulinate ester. The first step in chitin liquefaction is the depolymerization of a chitin polymer chain by EG to produce EG-derived NAG units (HAADP), which is comparable to the behavior of cellulose. However, decomposition of HAADP was not observed. Instead, the acetyl amide group hydrolyzed to form HADP. Such a two-step reaction scheme, i.e., formation of HAADP via solvolysis followed by sequential hydrolysis, was supported by FTIR analysis. Negligible deacetylation occurred on the polymer chain in
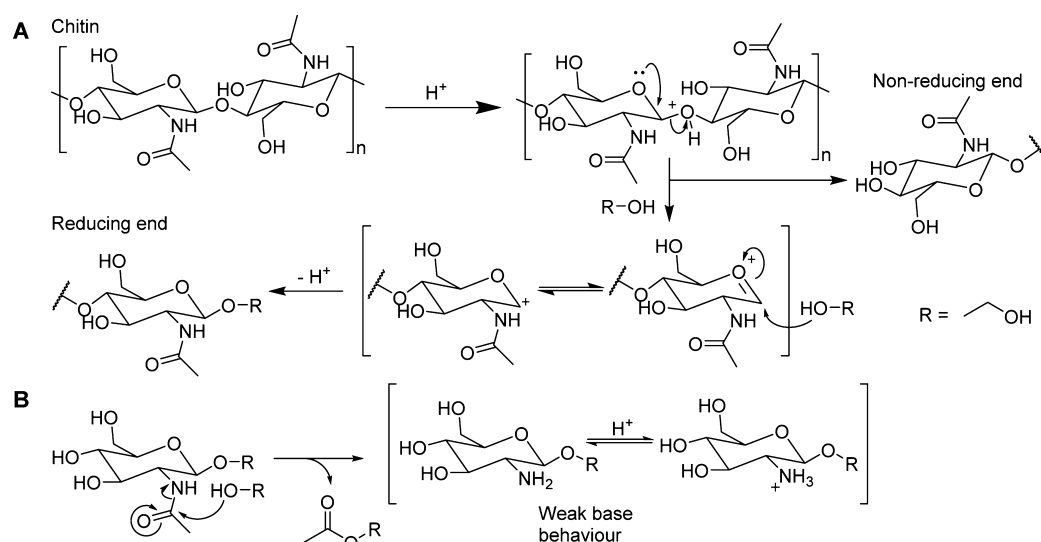
Figure 10. Proposed reaction pathways for chitin liquefaction: initial solvolysis (A) and sequential deacetylation (B).

the FTIR spectra of recovered chitin, demonstrating that the hydrolysis of acetyl amide takes place after the formation of HAADP. On the basis of the product identification and kinetic study, a reasonable pathway was proposed for chitin liquefaction (Figure 10). The cleavage of the glycosidic bond is achieved by the formation of an oxonium intermediate in the presence of acid increasing the electrophilicity on the C1 position. Then, a nucleophilic attack from the hydroxyl group of EG takes place to break up the C—O bond and form HAADP. Afterward, the side chain could easily be solvolyzed after activation of the amide by the acid to afford HADP and 2-hydroxyethyl acetate.[68] Other products such as the oligomers and a trace amount of glucosamine are likely to form in the hydrolysis reaction of chitin.

CONCLUSION

The liquefaction of chitin in EG has been demonstrated for the first time. Up to 75% of chitin was converted under the catalysis of sulfuric acid in EG solvent at 165 °C within 90 min. A fractionation procedure was employed for product separation and identification. By using the silylation reaction coupled with GC-MS analysis, the major products were identified as HADP and HAADP, both of which are derivatives of chitin monosugar, with a total yield of more than 30%. HPLC purification combined with NMR analysis further confirmed the structure of HAADP. A kinetic study and FTIR analysis suggested that chitin underwent solvolysis to form HAADP, followed by the deacetylation reaction to afford HADP. Interestingly, the structural evolution of chitin residues by XRD analysis showed that the crystallinity of chitin decreased significantly after liquefaction. The simple, cheap, and efficient liquefaction of chitin opens up a new route to produce N-containing chemicals and materials from waste in the fishing industry.

ASSOCIATED CONTENT

Ⓢ Supporting Information

Analysis such as NMR data, GC-MS spectrum of blank experiment, and others. This material is available free of charge via the Internet at http://pubs.acs.org.

AUTHOR INFORMATION

Corresponding Author

*E-mail: ning.yan@nus.edu.sg.

Author Contributions

Y. Pierson and X. Chen contributed equally to this work.

Notes

The authors declare no competing financial interest.

ACKNOWLEDGMENTS

REFERENCES

(1) Somerville, C.; Youngs, H.; Taylor, C.; Davis, S. C.; Long, S. P. Feedstocks for lignocellulosic biofuels. *Science* **2010**, *329*, 790−792.

(2) Rostrup-Nielsen, J. R. Making fuels from biomass. *Science* **2005**, *308*, 1421−1422.

(3) Corma, A.; Iborra, S.; Velty, A. Chemical routes for the transformation of biomass into chemicals. *Chem. Rev.* **2007**, *107*, 2411−2502.

(4) Kumar, M. N. V. R. A review of chitin and chitosan applications. *React. Funct. Polym.* **2000**, *46*, 1−27.

(5) Yan, N.; Dyson, P. J. Transformation of biomass via the selective hydrogenolysis of CO bonds by nanoscale metal catalysts. *Curr. Opin. Chem. Eng.* **2013**, *2*, 178−183.

(6) Zakzeski, J.; Bruijnincx, P. C. A.; Jongerius, A. L.; Weckhuysen, B. M. The catalytic valorization of lignin for the production of renewable chemicals. *Chem. Rev.* **2010**, *110*, 3552−3599.

(7) Siankevich, S.; Fei, Z.; Scopelliti, R.; Laurenczy, G.; Katsyuba, S.; Yan, N.; Dyson, P. J. Enhanced conversion of carbohydrates to the platform chemical 5-hydroxymethylfurfural using designer ionic liquids. *ChemSusChem* **2014**, *7*, 1647−1654.

(8) Shi, N.; Liu, Q.; Wang, T.; Ma, L.; Zhang, Q.; Zhang, Q. One-pot degradation of cellulose into furfural compounds in hot compressed steam with dihydric phosphates. *ACS Sustainable Chem. Eng.* **2014**, *2*, 637−642.

(9) Kobayashi, H.; Fukuoka, A. Synthesis and utilisation of sugar compounds derived from lignocellulosic biomass. *Green Chem.* **2013**, *15*, 1740−1763.

(10) Yan, N.; Zhao, C.; Luo, C.; Dyson, P. J.; Liu, H.; Kou, Y. One-step conversion of cellobiose to C6-alcohols using a ruthenium nanocluster catalyst. *J. Am. Chem. Soc.* **2006**, *128*, 8714−8715.

(11) Kobayashi, H.; Yabushita, M.; Komanoya, T.; Hara, K.; Fujita, I.; Fukuoka, A. High-yielding one-pot synthesis of glucose from cellulose

2087

dx.doi.org/10.1021/sc500334b | ACS Sustainable Chem. Eng. 2014, 2, 2081−2089

using simple activated carbons and trace hydrochloric acid. *ACS Catal.* **2013**, *3*, 581−587.

(12) Siankevich, S.; Savoglidis, G.; Fei, Z.; Laurenczy, G.; Alexander, D. T. L.; Yan, N.; Dyson, P. J. A novel platinum nanocatalyst for the oxidation of 5-hydroxymethylfurfural into 2,5-furandicarboxylic acid under mild conditions. *J. Catal.* **2014**, *315*, 67−74.

(13) Gürbüz, E. I.; Gallo, J. M. R.; Alonso, D. M.; Wettstein, S. G.; Lim, W. Y.; Dumesic, J. A. Conversion of hemicellulose into furfural using solid acid catalysts in γ-valerolactone. *Angew. Chem., Int. Ed.* **2013**, *52*, 1270−1274.

(14) Zhang, J.; Teo, J.; Chen, X.; Asakura, H.; Tanaka, T.; Teramura, K.; Yan, N. A series of NiM (M = Ru, Rh, and Pd) bimetallic catalysts for effective lignin hydrogenolysis in water. *ACS Catal.* **2014**, *4*, 1574−1583.

(15) Zhang, J.; Asakura, H.; van Rijn, J.; Yang, J.; Duchesne, P.; Zhang, B.; Chen, X.; Zhang, P.; Saeys, M.; Yan, N. Highly efficient, NiAu-catalyzed hydrogenolysis of lignin into phenolic chemicals. *Green Chem.* **2014**, *16*, 2432−2437.

(16) Chatel, G.; Rogers, R. D. Review: Oxidation of lignin using ionic liquids—An innovative strategy to produce renewable chemicals. *ACS Sustainable Chem. Eng.* **2013**, *2*, 322−339.

(17) Gao, Y.; Zhang, J.; Chen, X.; Ma, D.; Yan, N. A metal-free, carbon-based catalytic system for the oxidation of lignin model compounds and lignin. *ChemPlusChem* **2014**, *79*, 825−834.

(18) Zhao, Y.; Yan, N.; Feng, M. W. Biobased phenol formaldehyde resins derived from beetle-infested pine barks—Structure and composition. *ACS Sustainable Chem. Eng.* **2012**, *1*, 91−101.

(19) Kuo, P.-Y.; Sain, M.; Yan, N. Synthesis and characterization of an extractive-based bio-epoxy resin from beetle infested Pinus contorta bark. *Green Chem.* **2014**, *16*, 3483−3493.

(20) Zhao, Y.; Yan, N.; Feng, M. Polyurethane foams derived from liquefied mountain pine beetle-infested barks. *J. Appl. Polym. Sci.* **2012**, *123*, 2849−2858.

(21) Hayes, D. J. An examination of biorefining processes, catalysts and challenges. *Catal. Today* **2009**, *145*, 138−151.

(22) Lee, S. H.; Teramoto, Y.; Shiraishi, N. Biodegradable polyurethane foam from liquefied waste paper and its thermal stability, biodegradability, and genotoxicity. *J. Appl. Polym. Sci.* **2002**, *83*, 1482−1489.

(23) Kumar, P.; Barrett, D. M.; Delwiche, M. J.; Stroeve, P. Methods for pretreatment of lignocellulosic biomass for efficient hydrolysis and biofuel production. *Ind. Eng. Chem. Res.* **2009**, *48*, 3713−3729.

(24) Wei, Y.; Cheng, F.; Li, H.; Yu, J. Synthesis and properties of polyurethane resins based on liquefied wood. *J. Appl. Polym. Sci.* **2004**, *92*, 351−356.

(25) Kishi, H.; Fujita, A.; Miyazaki, H.; Matsuda, S.; Murakami, A. Synthesis of wood-based epoxy resins and their mechanical and adhesive properties. *J. Appl. Polym. Sci.* **2006**, *102*, 2285−2292.

(26) Hu, S.; Luo, X.; Li, Y. Polyols and polyurethanes from the liquefaction of lignocellulosic biomass. *ChemSusChem* **2014**, *7*, 66−72.

(27) Yamada, T.; Ono, H. Characterization of the products resulting from ethylene glycol liquefaction of cellulose. *J. Wood Sci.* **2001**, *47*, 458−464.

(28) Ferhan, M.; Tanguy, N.; Yan, N.; Sain, M. Comparison of enzymatic, alkaline, and UV/H$_2$O$_2$ treatments for extraction of beetle-infested lodgepole pine (BILP) and aspen bark polyphenolic extractives. *ACS Sustainable Chem. Eng.* **2013**, *2*, 165−172.

(29) D'Souza, J.; Yan, N. Producing bark-based polyols through liquefaction: Effect of liquefaction temperature. *ACS Sustainable Chem. Eng.* **2013**, *1*, 534−540.

(30) Kurimoto, Y.; Koizumi, A.; Doi, S.; Tamura, Y.; Ono, H. Wood species effects on the characteristics of liquefied wood and the properties of polyurethane films prepared from the liquefied wood. *Biomass Bioenergy* **2001**, *21*, 381−390.

(31) Yamada, T.; Aratani, M.; Kubo, S.; Ono, H. Chemical analysis of the product in acid-catalyzed solvolysis of cellulose using polyethylene glycol and ethylene carbonate. *J. Wood Sci.* **2007**, *53*, 487−493.

(32) Jasiukaitytė, E.; Kunaver, M.; Strlič, M. Cellulose liquefaction in acidified ethylene glycol. *Cellulose* **2009**, *16*, 393−405.

(33) Hu, S.; Wan, C.; Li, Y. Production and characterization of biopolyols and polyurethane foams from crude glycerol based liquefaction of soybean straw. *Bioresour. Technol.* **2012**, *103*, 227−233.

(34) Kobayashi, M.; Asano, T.; Kajiyama, M.; Tomita, B. Analysis on residue formation during wood liquefaction with polyhydric alcohol. *J. Wood Sci.* **2004**, *50*, 407−414.

(35) Yoshioka, M.; Nishio, Y.; Saito, D.; Ohashi, H.; Hashimoto, M.; Shiraishi, N. Synthesis of biopolyols by mild oxypropylation of liquefied starch and its application to polyurethane rigid foams. *J. Appl. Polym. Sci.* **2013**, *130*, 622−630.

(36) Hishikawa, Y.; Yamaguchi, M.; Kubo, S.; Yamada, T. Direct preparation of butyl levulinate by a single solvolysis process of cellulose. *J. Wood Sci.* **2013**, *59*, 179−182.

(37) Rinaudo, M. Chitin and chitosan: Properties and applications. *Prog. Polym. Sci.* **2006**, *31*, 603−632.

(38) Kerton, F. M.; Liu, Y.; Omari, K. W.; Hawboldt, K. Green chemistry and the ocean-based biorefinery. *Green Chem.* **2013**, *15*, 860−871.

(39) Yannas, I. V.; Burke, J. F.; Orgill, D. P.; Skrabut, E. M. Wound tissue can utilize a polymeric template to synthesize a functional extension of skin. *Science* **1982**, *215*, 174−176.

(40) Krajewska, B. Application of chitin- and chitosan-based materials for enzyme immobilizations: A review. *Enzyme Microb. Technol.* **2004**, *35*, 126−139.

(41) Uhrich, K. E.; Cannizzaro, S. M.; Langer, R. S.; Shakesheff, K. M. Polymeric systems for controlled drug release. *Chem. Rev.* **1999**, *99*, 3181−3198.

(42) Gadd, G. M. Biosorption: critical review of scientific rationale, environmental importance and significance for pollution treatment. *J. Chem. Technol. Biot.* **2009**, *84*, 13−28.

(43) Zia, K. M.; Barikani, M.; Zuber, M.; Bhatti, I. A.; Sheikh, M. A. Molecular engineering of chitin based polyurethane elastomers. *Carbohyd. Polym.* **2008**, *74*, 149−158.

(44) Sashiwa, H.; Shigemasa, Y. Chemical modification of chitin and chitosan 2: Preparation and water soluble property of N-acylated or N-alkylated partially deacetylated chitins. *Carbohyd. Polym.* **1999**, *39*, 127−138.

(45) Metreveli, A. K.; Metreveli, P. K.; Makarov, I. E.; Ponomarev, A. V. Aromatic products of radiation-thermal degradation of lignin and chitin. *High Energy Chem.* **2013**, *47*, 35−40.

(46) Einbu, A.; Vårum, K. M. Characterization of chitin and its hydrolysis to GlcNAc and GlcN. *Biomacromolecules* **2008**, *9*, 1870−1875.

(47) Vaaje-Kolstad, G.; Westereng, B.; Horn, S. J.; Liu, Z.; Zhai, H.; Sørlie, M.; Eijsink, V. G. H. An oxidative enzyme boosting the enzymatic conversion of recalcitrant polysaccharides. *Science* **2010**, *330*, 219−222.

(48) Yoon, J. H. Enzymatic synthesis of chitooligosaccharides in organic cosolvents. *Enzyme Microb. Technol.* **2005**, *37*, 663−668.

(49) Chen, F.; Lu, Z. Liquefaction of wheat straw and preparation of rigid polyurethane foam from the liquefaction products. *J. Appl. Polym. Sci.* **2009**, *111*, 508−516.

(50) Yan, Y.; Pang, H.; Yang, X.; Zhang, R.; Liao, B. Preparation and characterization of water-blown polyurethane foams from liquefied cornstalk polyol. *J. Appl. Polym. Sci.* **2008**, *110*, 1099−1111.

(51) Lee, W.-J.; Lin, M.-S. Preparation and application of polyurethane adhesives made from polyhydric alcohol liquefied Taiwan acacia and China fir. *J. Appl. Polym. Sci.* **2008**, *109*, 23−31.

(52) Mascal, M.; Nikitin, E. B. Dramatic advancements in the saccharide to 5-(chloromethyl)furfural conversion reaction. *ChemSusChem* **2009**, *2*, 859−861.

(53) Omari, K. W.; Besaw, J. E.; Kerton, F. M. Hydrolysis of chitosan to yield levulinic acid and 5-hydroxymethylfurfural in water under microwave irradiation. *Green Chem.* **2012**, *14*, 1480−1487.

(54) Wang, Y.; Pedersen, C. M.; Deng, T.; Qiao, Y.; Hou, X. Direct conversion of chitin biomass to 5-hydroxymethylfurfural in concentrated ZnCl$_2$ aqueous solution. *Bioresour. Technol.* **2013**, *143*, 384−390.

2088

dx.doi.org/10.1021/sc500334b | *ACS Sustainable Chem. Eng.* 2014, 2, 2081−2089

(55) Chen, X.; Chew, S. L.; Kerton, F. M.; Yan, N. Direct conversion of chitin into a N-containing furan derivative. *Green Chem.* **2014**, *16*, 2204−2212.

(56) Osada, M.; Kikuta, K.; Yoshida, K.; Totani, K.; Ogata, M.; Usui, T. Non-catalytic synthesis of Chromogen I and III from N-acetyl-D-glucosamine in high-temperature water. *Green Chem.* **2013**, *15*, 2960−2966.

(57) Focher, B.; Beltrame, P. L.; Naggi, A.; Torri, G. Alkaline N-deacetylation of chitin enhanced by flash treatments. Reaction kinetics and structure modifications. *Carbohyd. Polym.* **1990**, *12*, 405−418.

(58) Kasaai, M. R. A review of several reported procedures to determine the degree of N-acetylation for chitin and chitosan using infrared spectroscopy. *Carbohyd. Polym.* **2008**, *71*, 497−508.

(59) Langer, S. H.; Connell, S.; Wender, I. Preparation and properties of trimethylsilyl ethers and related compounds. *J. Org. Chem.* **1958**, *23*, 50−58.

(60) Scanlon, J. T.; Willis, D. E. Calculation of flame ionization detector relative response factors using the effective carbon number concept. *J. Chromatogr. Sci.* **1985**, *23*, 333−340.

(61) DeJongh, D. C.; Radford, T.; Hribar, J. D.; Hanessian, S.; Bieber, M.; Dawson, G.; Sweeley, C. C. Analysis of trimethylsilyl derivatives of carbohydrates by gas chromatography and mass spectrometry. *J. Am. Chem. Soc.* **1969**, *91*, 1728−1740.

(62) Medeiros, P. M.; Simoneit, B. R. T. Analysis of sugars in environmental samples by gas chromatography−mass spectrometry. *J. Chromatogr. A* **2007**, *1141*, 271−278.

(63) Wang, H.; Chen, H.-Z. A novel method of utilizing the biomass resource: Rapid liquefaction of wheat straw and preparation of biodegradable polyurethane foam (PUF). *J. Chin. Inst. Chem. Eng.* **2007**, *38*, 95−102.

(64) Osada, M.; Miura, C.; Nakagawa, Y. S.; Kaihara, M.; Nikaido, M.; Totani, K. Effects of supercritical water and mechanochemical grinding treatments on physicochemical properties of chitin. *Carbohyd. Polym.* **2013**, *92*, 1573−1578.

(65) Pearson, F. G.; Marchessault, R. H.; Liang, C. Y. Infrared spectra of crystalline polysaccharides. V. Chitin. *J. Polym. Sci.* **1960**, *43*, 101−116.

(66) Zhang, H.; Ding, F.; Luo, C.; Xiong, L.; Chen, X. Liquefaction and characterization of acid hydrolysis residue of corncob in polyhydric alcohols. *Ind. Crops Prod.* **2012**, *39*, 47−51.

(67) Lee, S.-H.; Yoshioka, M.; Shiraishi, N. Liquefaction of corn bran (CB) in the presence of alcohols and preparation of polyurethane foam from its liquefied polyol. *J. Appl. Polym. Sci.* **2000**, *78*, 319−325.

(68) Cho, Y. W.; Jang, J.; Park, C. R.; Ko, S. W. Preparation and solubility in acid and water of partially deacetylated chitins. *Biomacromolecules* **2000**, *1*, 609−614.